Biomass Conversion and Biorefinery
https://doi.org/10.1007/s13399-025-06907-9

ORIGINAL ARTICLE

Adsorption capacity of nanocomposite synthesized using biochar sourced from *Telfairia occidentalis* stem and titanium oxide for the removal of acetaminophen

James Friday Amaku[1] · Okoche Kelvin Amadi[2] · Fanyana M. Mtunzi[1] · Jesse Greener[3]

Received: 12 January 2025 / Revised: 15 April 2025 / Accepted: 12 August 2025

Abstract
The study aimed to assess the effectiveness of TiO_2/ZnO nanocomposite-modified biochar (TZB) derived from pristine biochar (TBC) precursor materials to sequester acetaminophen (APH) from the aqueous solution using the batch adsorption technique. The uptake of APH by TZB and TBC was examined at solution pH 7, 30 mg adsorbent dose, and a 100-min contact time. The findings suggest a bimolecular interaction between the adsorbates and adsorbents, with pseudo-second-order kinetics. According to isotherm research, Langmuir and Freundlich models, respectively, best fit the data acquired for TZB and TBC. For both TBC and TZB, an increase in the Langmuir monolayer adsorption parameters was observed, suggesting better sorption of acetaminophen with increasing solution temperature. According to thermodynamic studies, both adsorbents spontaneously removed acetaminophen. Acetaminophen elimination by TBC and TZB was an endothermic procedure. This study validates the prospective use of TBC and TZB as potential capacity substitutes for treating pharmaceutical-polluted wastewater.

Keywords Acetaminophen · *Telfairia occidentalis* · Nanocomposite · Biochar · Antimicrobial · Regeneration

1 Introduction

The identification of emerging environmental contaminants (ECs) in wastewater and aquatic environments is increasing [1]. Interestingly, some of these ECs degrade to form intermediate of unknown chemistry and these substances are receiving a lot of attention since they may have harmful effects on human health and the environment [1]. Pharmaceuticals and other toxic industrial chemicals that are discharged as effluents are examples of mixed families of substances that are considered ECs [2]. Acetaminophen is extensively used as a fever reducer and pain reliever with a global production of approximately a million tonnes per year [2]. Hence, the detection of this EC is becoming more prevalent in groundwater and wastewater treatment plants [3]. The quantity of acetaminophen in any water body or effluent is largely dependent on the source of the contaminant [3]. A previous study reported acetaminophen concentrations as high as 10 mg dm^{-3} in wastewater treatment plant effluents [4, 5]. In addition, 427 ng/L was detected in surface water [6], whereas, on the contrary, hospital wastewater was found to contain a concentration of 1.35 mg dm^{-3} [7]. This shows the spread of this water contaminant across the different waterbodies.

Research efforts are increasingly focused on developing low-cost techniques for eliminating acetaminophen and other pollutants that are becoming increasingly problematic [8]. As adsorption removes the need for chemicals and additional steps to recover or manage possible toxic byproducts, it is the simplest and most economical wastewater treatment technique [9, 10]. The effectiveness of this process is largely dependent on the nature of the adsorbent employed [9, 11–13]. Adsorbents such as seed husk [14], graphene oxide [15], silica [16], activated carbon [17], chitosan [18], chars [19], multi-walled carbon nanotubes [20], metal–organic

✉ James Friday Amaku
fridaya@vut.ac.za

[1] Wastewater Treatment Research Laboratory, Department of Biotechnology and Chemistry, Vaal University of Technology, Vanderbijlpark, Gauteng 1911, South Africa

[2] Department of Chemistry, Michael Okpara University of Agriculture, Abia State, Umudike, Abia State P.M.B 7267, Nigeria

[3] Département de Chimie, Université Laval, Québec, QC G1V 0A6, Canada

Published online: 15 September 2025

frameworks [21], Fe_3O_4@C [22], nutshell [23], NPs [24], nanocomposite [25], bacteria [26], cellulose [27], hydrogel, and biochar [28] have been employed for the elimination of pharmaceuticals from wastewater.

Among the materials that have been used as adsorbents for the elimination of pharmaceuticals is biochar. Carbon-based materials having a turbostratic structure and a well-developed porous texture are generally termed biochar [29]. Biochar is commonly employed in energy storage gadgets, liquids and gas purification processes, catalysis, and electrochemical reactions [30]. Biochar is generally produced from a wide variety of precursors with high carbon contents via the pyrolytic method, among many other things, sawdust [31], leaf [32], stem [33], bio-waste [34], bone [35] and solid-waste [36] among others have been employed for the fabrication of biochar. Owing to its unique surface area and different chemical moieties on its surface it favours their interaction and analyte trapping capacity. Zinc oxide nanoparticles (ZnO NPs) have been extensively employed as nano-adsorbents [37, 38]. ZnO NPs have been established to be non-hazardous, biocompatible, chemically stable, and environmentally friendly [38]. Besides the aforementioned, ZnO NPs have demonstrated excellent antimicrobial activity [31].

The study aimed to fabricate TiO_2-impregnated/beta-cyclodextrin ZnO NPs decorated biochar as a capacity adsorbent for the sequestration of acetaminophen (APH) from simulated wastewater. The adsorptive parameters that are associated with equilibrium, kinetics, and thermodynamics were established in addition to the antioxidant and antimicrobial properties of the nanocomposite.

2 Materials and methods

Telfairia occidentalis (Ugwu) stems were sourced from a local market and restaurant in Umueze Umunumo in Ehime Mbano Local Government Area of Imo State, Nigeria. β-Cyclodextrin (99.5%), Acetaminophen (purity > 99%), zinc acetate dihydrate ($Zn(CH_3CO_2)_2{\cdot}2H_2O$, 98%), sulphuric acid ($H_2SO_4$, 98%), hydrochloric acid (HCl, 36%), sodium chloride (NaCl, 99%), nitric acid (HNO_3, 98%), ethanol (99.9%), acetone (99.9%) and sodium hydroxide (NaOH, 97%) were purchased from Sigma-Aldrich and used without further treatment.

2.1 Preparation of biochar

Telfairia occidentalis (Ugwu) stems were allowed to air dry for seven days. After that, the samples were ground with an electric blender. The pulverized *T. occidentalis* stems (10 g) were soaked in 0.1 M butyl titanate for 24 h and vacuum oven-dried. The titanium-loaded *T. occidentalis* stem and pristine *T. occidentalis* stem were pyrolyzed for 90 min at 450 ℃ in a tubular furnace with a restricted air supply. The resultant biochars Ti/TBC and TBC were then reduced to fine particle size and stored separately in airtight containers.

2.2 Nanocomposite synthesis

We prepared nanocomposite TiO_2/ZnO modified biochar (TZB) from pristine biochar (the biochar company, TBC) precursor materials. Briefly, a mixture of Ti/TBC (10 g) and zinc acetate dihydrate (0.124 mol) solution was prepared. Separately, 0.1 mol dm^{-3} NaOH was prepared. The mixture was filtered after contacting both solutions at room temperature and vigorously stirring them for two hours. The resulting product was then repeatedly rinsed with distilled water. The TZB nanocomposite obtained was sealed and stored in an airtight container for further study after being dried overnight at 105 °C.

2.3 Instrumentation

The Fourier transform infrared (FTIR) spectra of TBC, TBC-APH, TZB, and TZB-APH were taken within a frequency range of 400–4000 cm^{-1} using a Thermo-Nicolet-870 spectrophotometer, USA. The crystallinity of TBC and TZB was assessed by an X-ray diffractometer apparatus (Bruker, USA) using 44 mA, $\lambda = 1.54$ Å (Cu-Kα) and 40 kV. The SEM micrograph of TBC, TBC-APH, TZB, and TZB-APH were acquired using JSM-7500 F, JEOL, Tokyo, Japan. The pH point of zero charges of TBC and TZB was examined using the solid addition method [39]. The thermal behaviour of TZB and TBC were assessed using a PerkinElmer simultaneous thermal analyzer STA6000 instrument, USA.

2.4 Batch adsorption experiments

The implication of pH on the adsorption of acetaminophen onto TBC and TZB was investigated using initial concentrations of 50 mg dm^{-3}, 30 mg of TBC or TZB, and solution pH ranging from 2 to 12. After being agitated for a predetermined amount of time at 25 ℃, the suspensions were filtered, and the equilibrium concentration was acquired. The effect of the dose of adsorbent was examined by varying the amount of adsorbent (0.01, 0.02, 0.03, 0.04, 0.05, 0.06, 0.07, 0.08, 0.09, and 0.1 g) that was contacted with 50 mg dm^{-3} of acetaminophen. To investigate the mechanism of adsorption and establish the equilibrium time, the kinetic of acetaminophen adsorption onto TBC and TZB was carried out. About 50 mg of TBC and TZB were added in a stoppered amber glass bottle containing 25 cm^3 of aqueous solutions of acetaminophen with a starting concentration of 50 mg dm^{-3} adjusted to a predetermined pH. Thereafter, suspensions were agitated

over varied contact times (5, 10, 15, 20, 25, 30, 60, 90, 120, and 180 min) in a shaker at 120 rpm at room temperature. The influence of initial acetaminophen concentration (5–50 mg dm^{-3}) and adsorbate temperature (298, 303, 313, and 318 K) were also investigated using pH 7, 50 mg of TBC and TZB, and 180-min agitation period. The reusability of TBC and TZB was performed by washing the used adsorbent with an effective eluting agent, the procedure was repeated four times, each time the sample was reintroduced for adsorption in a new acetaminophen solution. Briefly, 0.04 g of TBC or TZB was contacted with 50 cm^3 of 200 mg dm^{-3} acetaminophen solution for 3 h at 25 ℃. Thereafter, 20 cm^3 of ethanol was used to elute the adsorbed acetaminophen, and the equilibrium concentration was established. The mixtures were filtered under gravity, and the residual concentration of acetaminophen ions in the filtrate was determined by UV–visible spectrophotometry (Shimadzu UV-3600) (λ = 273 nm). All experiments were conducted in duplicate. The uptake capacity (mg g^{-1}) and the removal efficiency (% adsorbed) of acetaminophen were calculated by using Eqs.(1) and (2), respectively:

$$q_e = \left(\frac{C_i - C_{eq}}{m}\right)V \tag{1}$$

$$\%adsorbed = \left(\frac{C_i - C_{eq}}{C_i}\right) \times 100 \tag{2}$$

where V is the volume of the acetaminophen solution (dm^3), m is the mass (g) of the adsorbent, C_i is the starting concentration of acetaminophen (mg dm^{-3}), and C_{eq} is the equilibrium concentration (mg dm^{-3}).

2.5 Kinetics and isotherms study

Adsorption kinetics and isotherm were assessed using a solution pH of 7, 0.03 g adsorbent dose, 25 cm^3 of acetaminophen solution, and 150 rpm shaking speed at room temperature. In the uptake kinetic assessments, the mixtures were contacted over a time interlude of 5 to 180 min. At the end of each desired contact time interval, the samples were filtered, and the residual concentration was determined. Experimental data obtained from the influence of time experiments were fitted into the pseudo-first-order [40], pseudo-second-order [41], intraparticle diffusion [42], and Elovich [43] kinetics models (see Table 1). The removal process was determined using acetaminophen concentrations between 5 and 50 mg dm^{--3} and the acquired data were fixed into Freundlich and Langmuir isotherm models (see Table 2). To ascertain how the adsorption process behaves thermodynamically, the isotherm study was repeated for four different temperatures (298, 303, 313, and 318 K).

Table 1 Kinetics models used to assess the uptake of acetaminophen onto TBC and TZB

Kinetic models	Equations	Parameters	References
Pseudo-first order	$\frac{dq_t}{d_t} = k_1(q_e - q_t)$	k_1, q_e	[40]
Pseudo-second order	$\frac{dq_t}{d_t} = k_2(q_e - q_t)^2$	k_2, q_e	[41]
Weber-Morris intra-particle diffusion	$\frac{dq_t}{d_{t-0.5}} = k_{id}$	k_{id}, l	[42]
Elovich	$\frac{dq_t}{d_t} = \alpha e^{(-\beta q_t)}$	α, β	[43]

α, adsorption rate constant (mg g^{-1} min^{-1}); k_1, pseudo-first order rate constant (min^{-1}); k_2, pseudo-second order rate constant (g mg^{-1} min^{--1}); k_{id}, intraparticle diffusion rate constant (mg g^{-1} $min^{0.5}$); q_e, quantity of adsorbate adsorbed at equilibrium (mg g^{-1}); q_t, quantity of adsorbate adsorbed at time t (mg g^{-1}); l, is a constant related to the boundary layer thickness (mg g^{-1}); β, desorption rate constant (g mg^{-1})

Table 2 Isotherm equations and parameters used to describe the uptake of acetaminophen onto TBC and TZB

Isotherm model	Equation	Parameters	References
Langmuir	$q_e = \frac{q_{max} b C_e}{1+bC_e} q_{max}$	b	[44]
Freundlich	$q_e = K_F C_e^{1/n}$	k_F, n	[45]

q_e, adsorption capacity (mg g^{-1}) of TBC or TZB; C_{eq}, equilibrium concentration of acetaminophen in solution (mg dm^{-3}); q_{max}, maximum monolayer adsorption capacity (mg g^{-1}) of TBC or TZB; b, Langmuir isotherm constant (dm^3 mg^{-1}); k_F, Freundlich isotherm constant (mg g^{-1}) (dm^{-3} $mg^{-1})^n$; n, adsorption intensity

2.6 Antioxidant assay

Using a 2,2-diphenyl-1-picrylhydrazyl (DPPH) assay, the antioxidant properties of TBC and TZB were evaluated. In summary, 0.5 cm^3 of a 0.3 mM DPPH solution was added to TBC or TZB at various concentrations (25, 50, 100, 200, and 400 g cm^{-1}). DPPH was used as a radical source, while the wastewater treatment agent (TBC and TZB) served as a radical scavenger. The mixture of the radical source and the radical scavengers was incubated for 30 min at 25 °C in a dark container. By utilizing the change in the percentage of absorption wavelength at 517 nm, the concentration of the radical was calculated and the level of inhibition (I%) of the DPPH was determined using Eq.(3) [46].

$$\%I = \frac{\left(\text{Asorbance}_{\text{control}} - \text{Asorbance}_{\text{Sample}}\right)}{\text{Asorbance}_{\text{control}}} \times 100 \tag{3}$$

2.7 Antibacterial activity

The antibacterial properties of TZB and TBC were evaluated using the Agar-well diffusion method. Ciprofloxacin served as a positive control to compare the effectiveness of the water treatment agents (TZB and TBZ) against gram-positive (*Staphylococcus aureus*) and gram-negative (*Escherichia coli*) bacteria. Microbial suspensions were plated onto Petri dishes with Muller-Hinton Agar. Wells, approximately 10 mm in diameter, were made in the agar using a well cutter, and 250 µg of TBC and TZB were added to each well. After incubating at 37 °C for 24 h, the antibacterial activity of TBC and BBC was determined by measuring the zone of inhibition around the wells.

2.8 pH point of zero charge (pH_{PZC})

About 0.1 g of TBC and TZB were put into eleven 250 cm^3 volumetric flasks, each holding 45 cm^3 of 0.1 mol dm^{-3} sodium chloride solution, in order to measure the pH at the point of zero charge of TBC and TZB, the mixture was then adjusted to pH values between 2 and 12. The flasks were sealed and agitated in a pre-heated water bath set to 25 °C for 48 h. After 48 h, the mixture's final pH was determined. The pH_{PZC} of TBC and TZB was then calculated from the line intercept by plotting the mixture's final pH against its initial pH [39].

2.9 Data analysis

The statistical computing environment of R utilized nonlinear regression routine technique to analyze the experimental data obtained for contact time and initial acetaminophen concentration experiment [47]. The R statistical software considers the minimization of both the sum of squared residuals (SSR) and the residual sum of errors (RSE). A comparison of all SSR and RSE values was performed, and the model adequacy was evaluated based on the value with the lowest SSR (A lower SSR is preferable because it signifies that the model's predictions are more accurate and closely align with the experimental data). The batch optimization data were plotted in Origin 2016 pro using error bars in all plots were obtained from the standard error of the mean, calculated from repeated experiments (duplicates). The analysis involved the application of empirical models and the estimated residuals of the models were used to validate the adequacy of the models.

3 Results and discussion

Figure 1 shows the SEM micrograph of TZB, TZB-APH, TBC, and TBC-APH. The pristine biochar (TBC) revealed irregular shapes of cracked chambers with rough edges. After the adsorption step, TBC-APH was noticed to have loosely packed particles with irregular structural shapes. The introduction of titanium and zinc nanoparticles as the surface modifier resulted in enhanced surface-coated characteristics. This indicates a compatible interaction between the surface of the biochar and the nanometals used as modifiers. In contrast, the spent TZB was observed to have a smooth surface, suggesting successful fixation of acetaminophen onto its surface. The surface morphology of TZB and TBC suggests beneficial qualities for efficient adsorption of acetaminophen.

The physicochemical variations on the surface of TBC after the modification step and the implications of the adsorbate interaction with the adsorbents (TZB and TBC) were investigated using FTIR spectroscopy (see Fig. 2). The spectra revealed characteristics vibrational bands (cm^{-1}) that were assigned to different functional (see Table 3) [48, 49]. Notably, after the modification of TBC, a marginal shift in some bands with variation in the intensity of some peaks helps to validate the successful fabrication of the nanocomposite (see Table 3). A comparison of the bands acquired for pristine and spent adsorbent revealed a shift in bands that are indicative of the active functional groups that are responsible for the sequestration of APH onto TBC and TZB.

The thermal behaviour of TZB and TBC was assessed by making use of thermo gravimetric analysis (TGA) and the thermo grams are displayed in Fig. 3. The thermogram acquired for TZB and TBC unveiled the degradation stages at different temperature and their corresponding weight loss. Thus, Fig. 3 revealed an ~ 10% loss in mass in the initial degradation stage of TZB and TBC occurred within the temperature ranges of 25–102 °C. This observed weight loss can be attributed to the loss of physically absorbed water. On the other hand, about 14% and 10% weight loss were observed for TZB and TBC in the second decomposition stage (110–400) °C, respectively, which we attribute to the thermal decomposition of hydroxyl and carboxyl-containing compounds [50]. Interestingly, about 18% (TZB) and 11% (TBC) weight loss was noticed for the third degradation stage (400–600 °C) and can be associated with the volatilization of inorganic materials. Thereafter, 41% and 38% residues were left behind by TZB and (TBC) respectively. The slightly higher residual content of TZB confirms the successful incorporation of the nanometal into the biochar. Additionally, this study highlights the exceptional thermal stability and structural integrity of TZB, further demonstrating its robustness and capacity absorption capacity for advanced applications in systems with elevated temperature.

The XRD diffractograms of TBC and TZB nanocomposite are presented in Fig. 4. The XRD pattern of the prepared TBC was compared to that of TZB. The pristine biochar (TBC) showed peaks at 23.23° and 43.0°, these peaks correspond to the reflection (002) crystal plane of amorphous

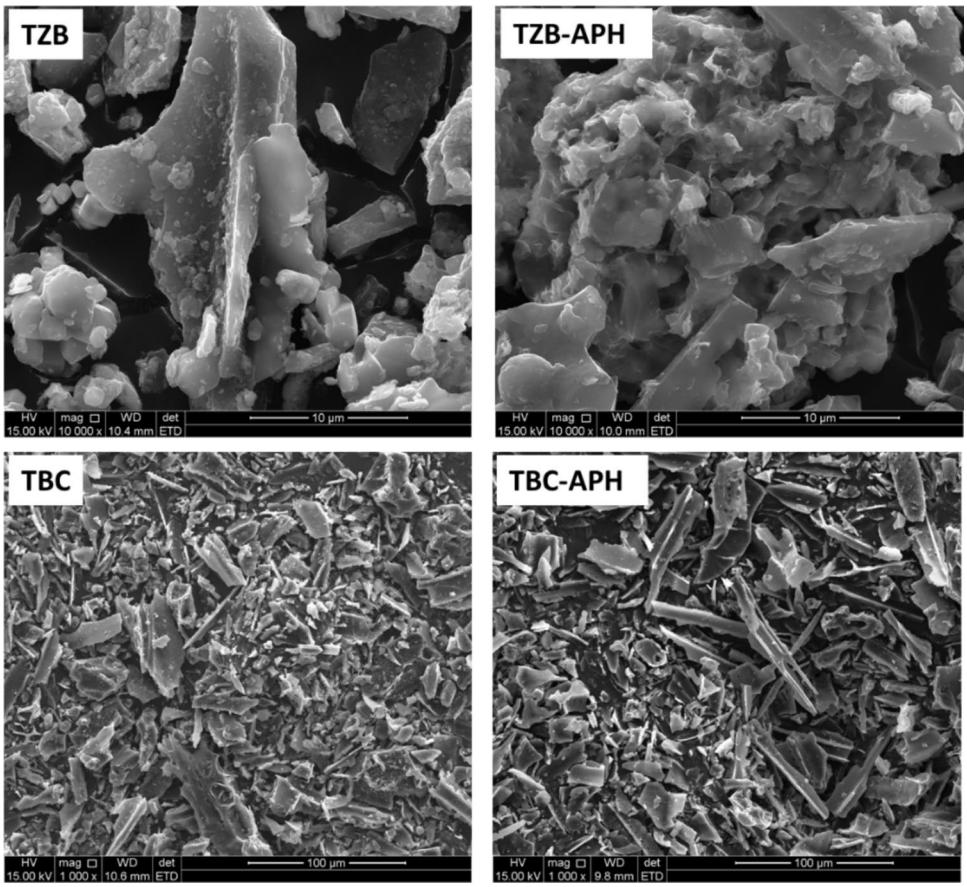

Fig. 1 SEM images of TZB, TZB-APH, TBC, and TBC-APH

carbon and the (100) plane of the graphitic structure. On the other hand, TZB was noticed to have peaks at 32.1, 34.2, 36.6, 47.7, 55.8, 63.1, 68.1° that corresponds to (100)Zn, (101)Zn, (004)Ti, (200)Ti, (105)Ti, (201)Zn, (103)Zn. The peak and their corresponding plane were consistent with JCPDS card no. 01–075-0576 for Zn and the standard card JCPDS No. 21–1272 the crystallographic planes of TiO_2 anatase phase. The mixed peaks and the nonappearance of some characteristic peaks suggest a semi-crystalline structure, it also indicates that TZB was successfully synthesized.

3.1 Effect of pH

The effect of pH on the removal of acetaminophen by TZB and TBC is illustrated in Fig. 5. The TZB and TBC uptake capacity increased when the solution pH increased from 1.0 to 6.0 and attained a maximum at pH 7.0. The TZB exhibited the highest acetaminophen removal, attaining ~ 49 mg g^{-1} at pH 7.0, and then declined as the solution pH was further increased. The point of zero charge (pH_{PZC}) for TZB and TBC were estimated as 7.83 and 5.48, respectively (see Fig. 6). Hence, hydrophobic interactions could be a possible path via which acetaminophen was sequestered. Furthermore, π-π interactions may be used to produce intermolecular forces between acetaminophen and the sorbents since the adsorbents mostly include π-electrons that can interact with organic contaminants that contain aromatic rings. These processes clarify why neutral circumstances promote the adsorption of acetaminophen by TZB and TBC. The uptake of acetaminophen onto TZB and TBC is therefore attributed primarily to the interactions between neutral molecules of acetaminophen and the active sites of TZB and TBC via hydrogen interaction, π-π interactions, or pore entrapment [51]. This study is consistent with the observation made using different adsorbents [52].

3.2 Influence of dosage

The effect of adsorbent dose was assessed over a sorbent range of 10–100 mg. As revealed in Fig. 7**,** increasing the amounts of TBC and TZB with a constant concentration of acetaminophen resulted in enhanced efficiency of the adsorbents. The phenomenon is attributed to increases in the number of active sites available for adsorption, hence, adsorbate removal is enhanced. The incremental removal of acetaminophen continues until a point of equilibrium where its concentration becomes the limiting factor. Hence, the removal of acetaminophen was enhanced by increasing the adsorbent dose, obtaining better efficiencies by using TZB. It was observed that the removal

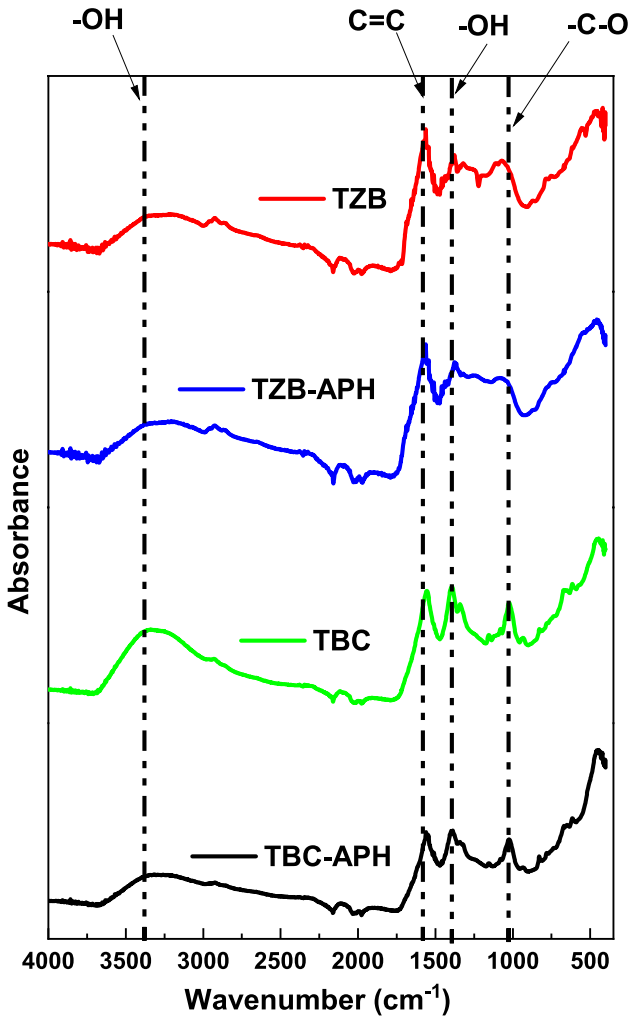

Fig. 2 FTIR spectra of TZB, TZB-APH, TBC, TBC-APH

Table 3 The observed FTIR spectral bands (cm^{-1}) and assignments

TZB	TZB-APH	TBC	TBC-APH	Assignments
3314	3298	3322	3346	υ(O–H, N–H)
1577	1567	1564	1564	C=C
1377	1372	1385	1385	υ_{bend}(O–H)
1059	1075	1019	1024	υ_{bend}(C-O)

capacity of acetaminophen was inversely proportional to the increase in the adsorbent amount from 10 to 100 mg. This owing to a significant amount of the adsorbent clumping together, which successfully lowers the saturation of the adsorption sites. In this study, a mass of 0.3 g was considered appropriate for adsorption, since effective comparison can be made at this dosage.

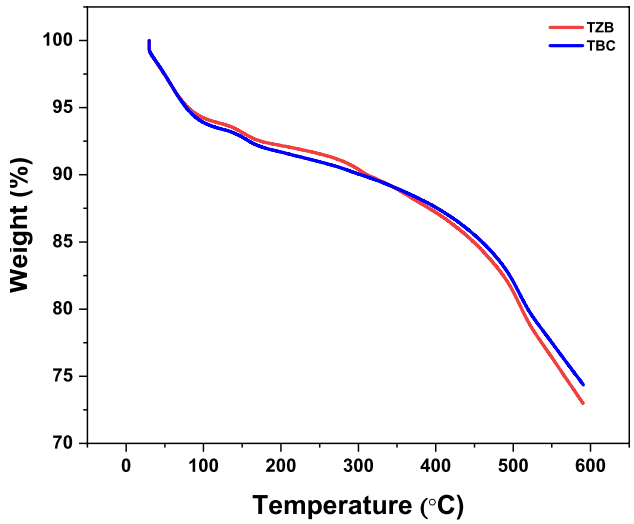

Fig. 3 The thermograms of TBC and TZB

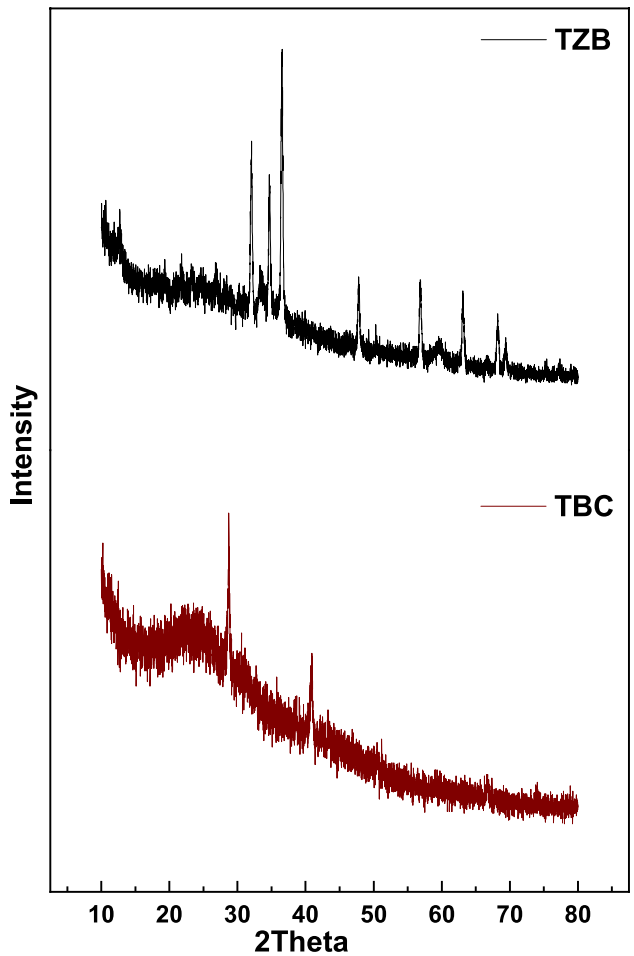

Fig. 4 XRD pattern of TZB and TBC

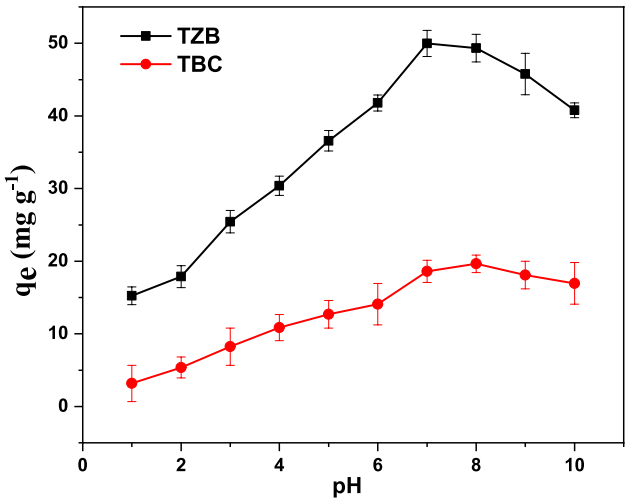

Fig. 5 The influence of solution pH on the ability of TBC and TZB to sequester acetaminophen from wastewater

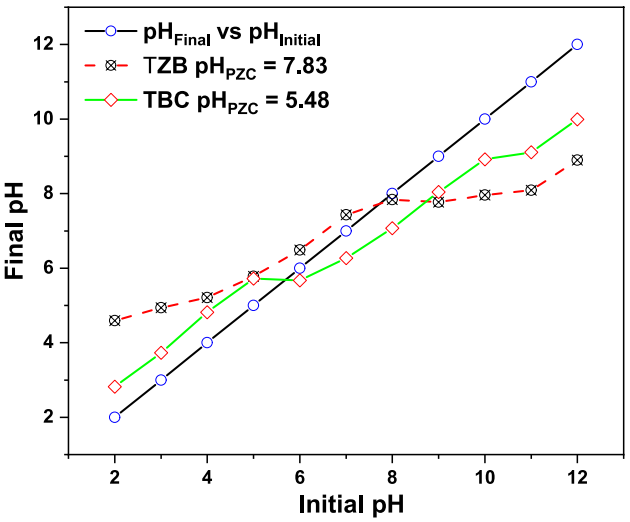

Fig. 6 Point of zero charge (pH_{PZC}) plots for TBC and TZB

3.3 Contact time

The influence of contact time on the adsorption of acetaminophen was assessed over a period of 5–180 min. As seen from Fig. 8, the capacity absorbance capacity for the removal of acetaminophen by TBC and TZB at different contact times (0 – 180 min). The figure demonstrated that with the increase in contact time, the adsorption capacity for the removal of acetaminophen increased significantly in the first 20 min for TBC and TZB. Further, an increase in contact time revealed a slow increase in the removal capacity of TBC and TZB and thereafter attained equilibrium within 100 min for the adsorbents. The sorption of acetaminophen onto TBC and TZB was rapid with a removal capacity of 15 mg g^{-1} and 48 mg g^{-1}, respectively after 100 min. This demonstrates that the incorporation of Ti into the biochar significantly improved the sorption ability of TZB, showing a high capacity for acetaminophen removal almost immediately in contact with the TZB. For further adsorption experiments, an agitation time of 180 min was employed for TBC and TZB to ensure the complete removal of acetaminophen from the solution.

3.4 Kinetic studies

A good understanding of the kinetic dynamics is essential to the design of large-scale adsorption technologies [53]. The mechanism for the uptake of acetaminophen onto TBC and TZB was assessed using the change in acetaminophen concentration as time (t) was varied. The data acquired were fitted into four kinetic models, namely, the pseudo-first order, pseudo-second order, Elovich, and intraparticle diffusion models. Table 1 illustrates the non-linear kinetic equations employed for the study. Table 4 displays the parameters estimated for the four models for acetaminophen adsorption onto TBC and TZB. Whereas Fig. 9 displayed the plots of the models for both TBC and TZB. The dependence of the model that best fits the experimental data was selected based on the one with the lowest SSR value. The adsorption of acetaminophen onto TBC and TZB was observed to have 5.366 and 298.1 as the least SSR values (see Table 4) that were assigned to the pseudo-second-order kinetic model. This indicates that the adsorption of acetaminophen onto TBC and TZB was adequately fit by a pseudo-second order model, this suggests that the rate-limiting step for the uptake of acetaminophen is via chemical interactions involving the sharing or exchange of electrons between the acetaminophen with TBC or TZB. Since the adsorption of acetaminophen onto the investigated adsorbents may be presumed to occur through hydrogen and/or π-π interactions, the results of this investigation further clarify the assertion. In these processes, π-electron-containing atoms on the active sites of TBC or TZB and the aromatic-ring electrons of acetaminophen may share electrons. Thus, suggesting that two binding active centres on TBC and TZB are responsible for the adsorption of acetaminophen.

3.5 Isotherm study

The removal capacity of acetaminophen in the initial concentrations range of 5–50 mg dm^{-3} was assessed using predetermined optimum conditions such as 180 min contact time, 30 mg adsorbent dose, solution pH 7, and 150 rpm at 298 K. The experiment was repeated using solution temperatures 303 K, 308 K, and 313 K. Thereafter, the implication of initial acetaminophen concentration at varied solution temperatures was assessed and presented in Fig. 10.

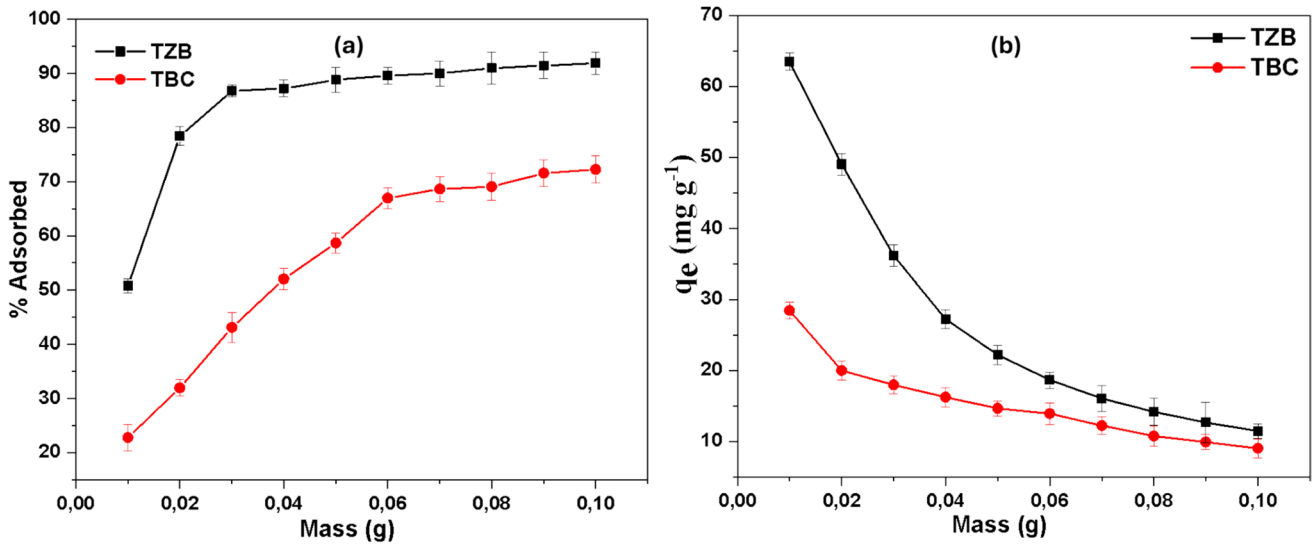

Fig. 7 The effect of mass of the adsorbent dosage on the sequestration acetaminophen by TBC and TZB as measured by (**a**) the % adsorbed and (**b**) the adsorption capacity

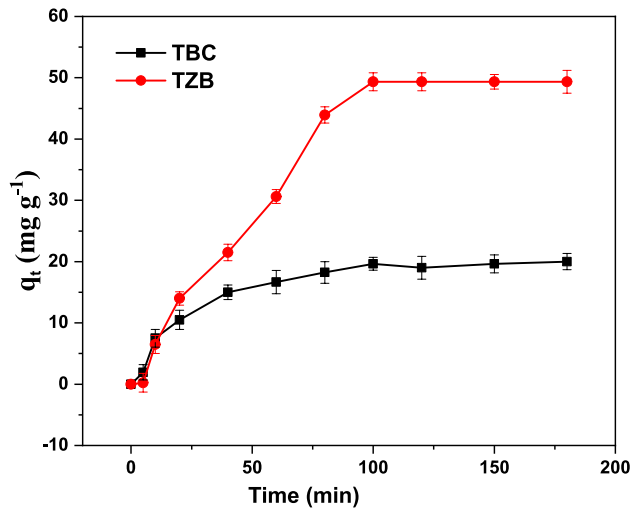

Fig. 8 Effect of contact time on the sequestration of acetaminophen by TBC and TZB as measured by the absorption capacity

Table 4 The estimated kinetic parameters for the uptake of acetaminophen onto TBC and TZB

Model	Parameter	TBC	TZB
Experimental	q_{exp} (mg g^{-1})	24.23	56.54
Pseudo first order	k_1(min^{-1})	0.037	0.013
	q_e (mg g^{-1})	19.57	60.16
	SSR	6.442	330.4
	RSE	0.819	6.015
Pseudo second order	k_2 (g mg^{-1} min^{-1})	0.002	9.9×10^{-5}
	q_e (mg g^{-1})	23.28	89.68
	SSR	5.366	298.1
	RSE	0.897	6.427
Intraparticle diffusion	k_{id} (mg g^{-1} $min^{-0.5}$)	1.798	4.061
	l (mg g^{-1})	-	-
	SSR	64.94	583.8
	RSE	2.686	8.054
Elovich	α (mg g^{-1} min^{-1})	−4.728	−32.23
	β (g mg^{-1})	5.053	16.23
	SSR	9.506	435.1
	RES	1.090	7.375

The increase in the uptake capacity of acetaminophen with increasing acetaminophen concentrations and solution temperature may be attributable to increased driving force due to enhanced concentration gradient. The mass transfer and diffusion of acetaminophen molecules onto the active sites of TBC and TZB were enhanced with an increase in solution temperature. Therefore, elevated temperatures led to a better elimination of acetaminophen (see Fig. 10). This suggests an endothermic process of adsorption was favoured. Considering the effectiveness of these adsorbents at room and elevated solution temperatures, the outcome shows that TBC and TZB could prove effective for the removal of acetaminophen regardless of adsorbate temperature. Consequently, they are appropriate for treating APH-polluted effluents directly before they are released into the water bodies.

Isotherms are required to set up an adsorption process that involves the removal of adsorbate on an industrial scale. The Langmuir and Freundlich isotherms were used to probe the adsorbate-adsorbent interaction using the acquired equilibrium data. The non-linear equations for every isotherm are given in Table 2. The isotherm with the lowest SSR value was chosen

.

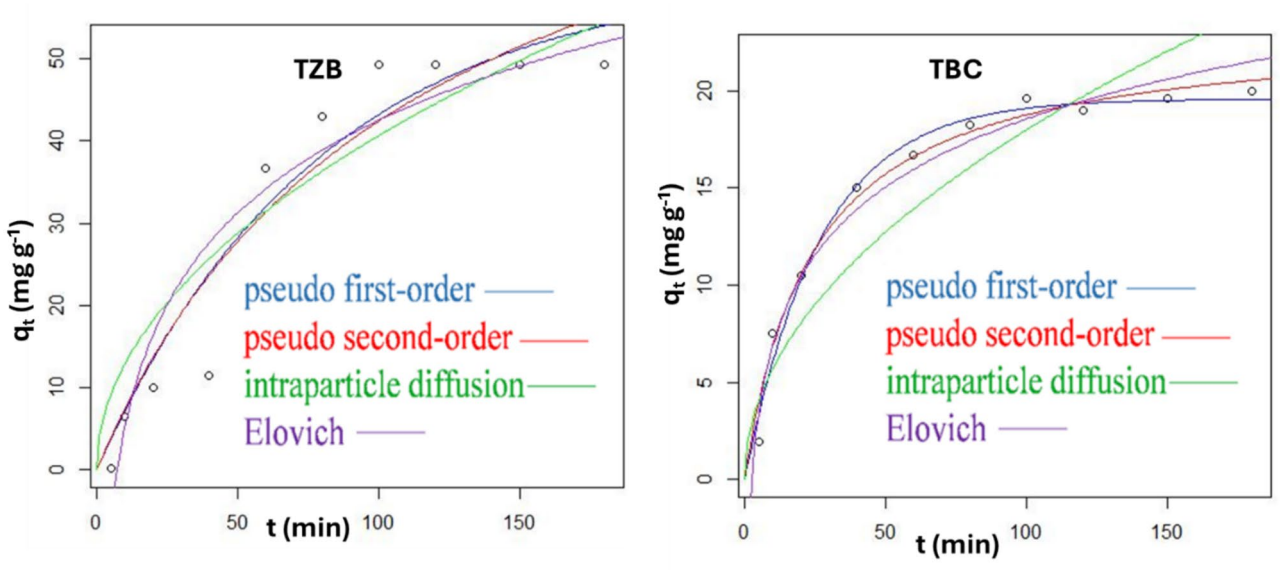

Fig. 9 Kinetic modelling of the adsorption of acetaminophen onto TBC and TZB based on measured time-varying absorbance capacity

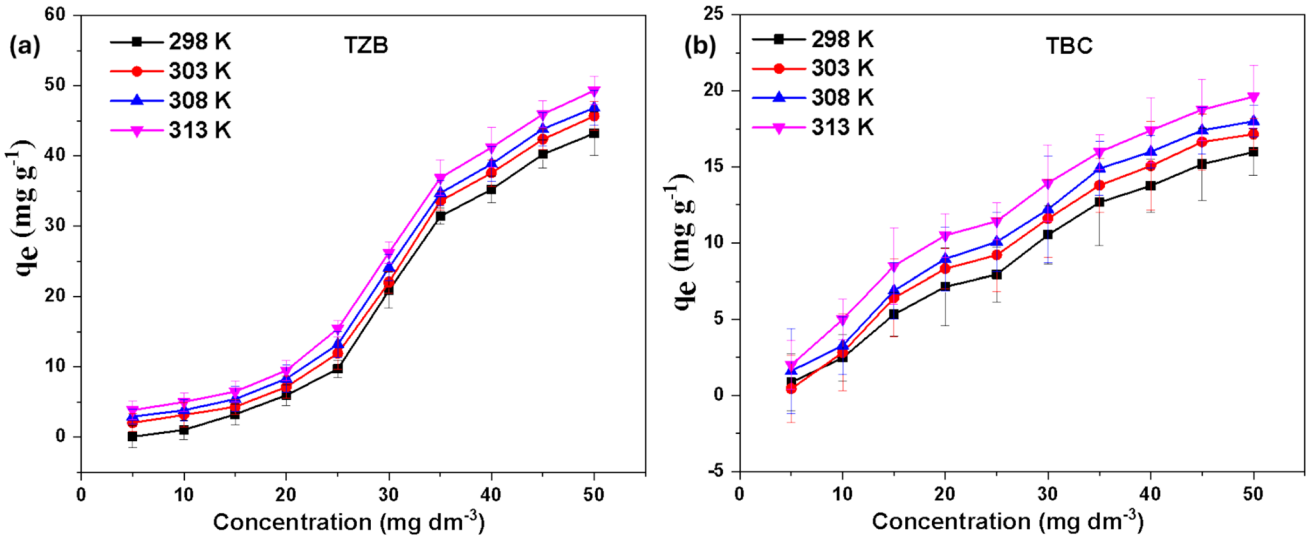

Fig. 10 The influence of adsorbate concentration on the absorbance capacity of acetaminophen by (**a**) TZB and (**b**) TBC

following a non-linear least squares (NLLS) analysis of each model. The features of the isotherms that best characterize the equilibrium data for the adsorption of acetaminophen are provided in Table 5. The optimum uptake capacity of TZB and TBC was demonstrated promising capacity when compared to previously used adsorbents(seeTable 6).Table 5 shows that the Freundlich and Langmuir models, respectively, provided a superior description of the equilibrium data collected for acetaminophen removal utilizing TZB and TBC. When compared to other models, the model with the least SSR values served as the basis for the deduction. The endothermic nature of acetaminophen sorption on the investigated adsorbents was demonstrated by the increase in the Freundlich sorption coefficient (k_F) and Langmuir maximum adsorption capacity (q_{max}) with increasing temperature. The Freundlich model assumes a heterogeneous surface and is therefore based on the multilayer adsorption of acetaminophen onto TZB. Conversely, the monolayer mechanism plays a crucial part in the adsorption process of acetaminophen onto TBC. Strong binding connections between the acetaminophen molecule and TZB or TBC were suggested by the observed rise in adsorptive power (b) with increasing temperature. The 1/n values were likewise less

Table 5 Adsorption isotherm model parameters for acetaminophen sequestration by TBC and TZB

Adsorbent	Isotherm	Parameters	Temperature			
			295 K	303 K	310 K	318 K
TZB	Freundlich	k_F	9.6349	11.033	12.0621	14.958
		n	3.5941	3.81583	3.927	4.6874
		SSR	2523	2757	5040	5071
	Langmuir	q_{max}	25.412	27.1957	39.0016	45.910
		b	0.2843	0.32037	0.6312	0.71248
		SSR	2462	2680	2795.4	2938
TBC	Freundlich	k_F	0.6889	0.75687	0.94785	1.32276
		n	1.1425	1.12976	1.1962	1.27949
		SSR	8.7901	15.662	15.255	22.529
	Langmuir	q_{max}	14.445	16.1429	16.5046	16.9324
		b	0.39199	0.51561	0. 7135	0.99628
		SSR	519.72	759.19	598.15	540.6

Table 6 Comparing the uptake capacity of the adsorbent used in this study with other adsorbents

Adsorbent type	Absorption capacity (mg g^{-1})	Reference
Activated carbon	118	[54]
NFO@SiO_2@APTS	49.00	[25]
Rh-cMNP	96.30	[55]
CAC	221.0	[52]
CANa1	20.96	[56]
Ca (II)-doped chitosan/β-cyclodextrin	200.86	[57]
TBC	16.93	This work
TZB	45.91	This work

Table 7 Thermodynamic factors for the absorption of acetaminophen onto TBC and TZB

Adsorbents	T (K)	ΔG° kJ mol^{-1}	ΔH kJ mol^{-1}	ΔS J K^{-1} mol^{-1}
TZB	298	− 20.2452	203.04	483.43
	303	− 22.3396		
	310	− 22.8557		
	318	− 25.476		
TBC	298	− 16.9788		
	303	− 19.1281	75.86	440.63
	310	− 20.8879		
	318	− 20.9625		

than 1, suggesting that TZB and TBC were used to remove acetaminophen in a favourable adsorption process.

3.6 Thermodynamic study

Sorbent-sorbate interaction is often accompanied by energy conversion [58]. The frequency of collision between acetaminophen molecule and TZB or TBC would increase with increased adsorbate temperature. Hence, the interaction of acetaminophen molecules with TZB and TBC can be better understood using the thermodynamic model. Thermodynamic parameters including standard Gibbs energy change ($\Delta G°$), standard enthalpy change ($\Delta H°$), and standard entropy change ($\Delta S°$) were estimated by performing the adsorption experiments at 298 K, 303 K, 308 K, and 313 K, by using Eqs. (6) and (5) [59, 60].

$$\triangle G° = -RT \ln K \tag{4}$$

$$\ln K = - \triangle H°/RT + \triangle S°/R \tag{5}$$

Table 4 presents thermodynamic parameters estimated for the adsorption of acetaminophen onto TZB and TBC. The negative values of $\Delta G°$ were noticed to increase with increasing solution temperature, suggesting a spontaneous and favourable process at higher adsorbate temperature (see Table 7). Positive values of $\Delta H°$ were estimated for the uptake of acetaminophen onto TBC and TZB. This suggests an endothermic process for the uptake of acetaminophen by TBC and TZB. In a similar trend, positive $\Delta S°$ values were obtained for the adsorption of acetaminophen onto TBC and TZB indicating increased disorder at the solid-solution interface.

3.7 Desorption studies

To reduce the re-release of sequestered contaminant into the environment, reusing adsorbents is a crucial process that prevents the introduction of secondary pollutants into the aquatic ecosystem. To prevent the re-introduction of pollutants via sorbate leaching from the surface of spent adsorbents, regenerating and reusing spent adsorbents was

examined. This was accomplished by weighing 50 mg of APH-loaded TBC or TZB into glass bottles with 20 cm^3 ethanol and stirring them for 1 h in a water bath with a thermostat. Following several adsorption–desorption cycles, the results showed a reasonably excellent reuse (efficiency) of the spent adsorbents. About 79% and 58% removal efficiency were sustained by TZB and TBC after the fourth cycle (see Fig. 11). This suggests that the adsorbents may be effective in real-world industrial settings, owing to it reusable tendency and its robust removal efficiency after several cycles.

3.8 Antioxidant activity

The antioxidant activity of TBC and TZB was investigated using the DPPH assay. Figure 12 shows that TZB has a higher level of antioxidant activity compared to TBC. The inhibitory efficiency of TBC and TZB was noticed to increase with an increase in the concentration of TBC or TZB. The disruption of an oxidation process using chemical constituents that are termed antioxidants is often accompanied by interception of the free radical formation path or the elimination of free radicals [61]. This process tends to confer some protective measures on biomolecules like fats, enzymes, proteins, and amino acids via the trapping of nascent oxygen within the intracellular system and in extension will prevent cell death [62, 63]. Interestingly, the magnitude of oxidative damage on natural macromolecules is generally assessed using DPPH assay. It is worth mentioning that, charge (electrons or protons) transfer activities within the valence space of the composite may aid the reduction of free radicals to stable molecules. Comparing the results, TZB was observed to have a higher inhibition than did TBC. This phenomenon could be attributed to the incorporation of TiO_2/ZnO NPs

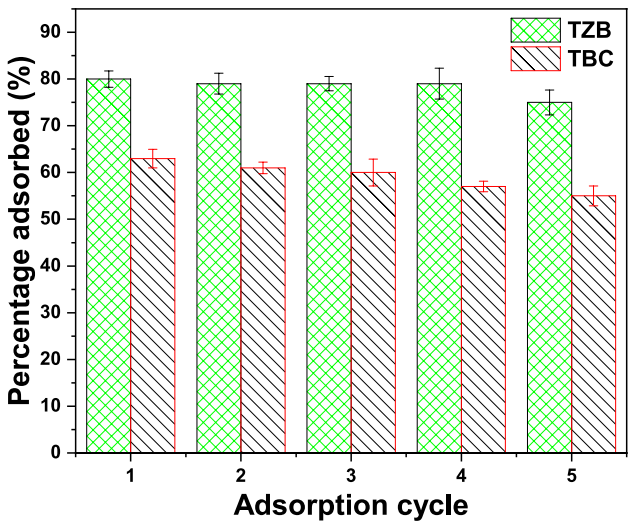

Fig. 11 Reusability of TBC and TZB for the removal of APH

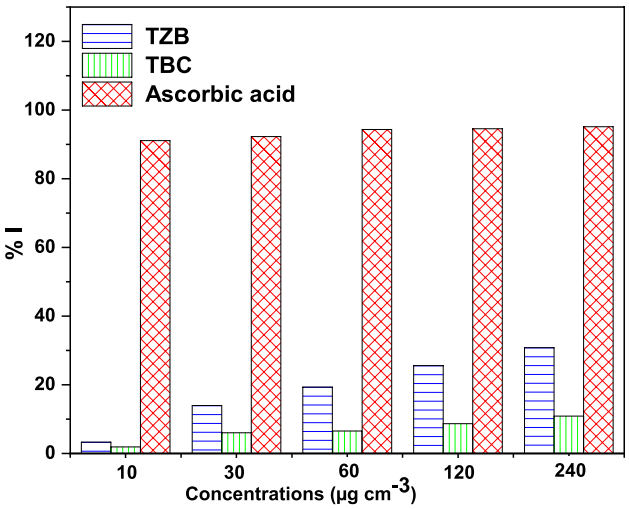

Fig. 12 Antioxidant activity of TBC or TZB

on the surface of the synthesized nanocomposite. Other authors reported similar results [64, 65].

3.9 Antibacterial activity

The antibacterial activity of TBC and TZB was investigated using gram-positive (*Staphylococcus aureus*) and gram-negative (*Escherichia coli*) strains of bacteria by measuring their zone of inhibition (mm). TZB and TBC with a concentration of 250 µg exhibited the maximum antibacterial activity against *E. coli* with the zone of inhibition of 2.1 mm and 1.5 mm, respectively. The synthesized TZB produced considerable zones of inhibition against *E. coli* than TBC. The observation indicates good antibacterial activity as shown in Table 8. This may be attributed to the incorporation of ZnO NPs into the biochar, which enhances the electron transfer characteristics of the composite, hence, the generation of active species by TZB may result in the damaged cellular membrane, leading to cell death. Hence, TZB has demonstrated superior bifunctional characteristics for diversified applications.

Table 8 Antimicrobial activity of TZB and TBC against *Staphylococcus aureusEscherichia coli*

Samples	Zone of inhibition (mm)	
	S. aureus	*E. coli*
TZB	R	2.1
TBC	R	1.5
Control	20.0	15.0

3.9.1 Cost estimation

The cost of acetaminophen removal by TZB was estimated using the material and operational costs. Briefly, the biomass used for the fabrication of the biochar was freely sourced (waste), hence accrued no cost ($0). Whereas, chemicals for the synthesis of nano-metals and reagent regents needed for adsorbent regeneration and pH adjustment were estimated to be ~ $150 per kg. operational cost which includes amber bottles, filter papers, and energy cost $0.20 per kWh) was estimated to be $20. Hence, the estimated cost per kg of the modified biochar: ~ $170 kg^{-1}. Consequently, optimum experimental factors of pH 7, 0.03 g adsorbent dosage, 180 min contact time and stirring rate 120 rpm suggest that 1 kg of TZB will be required to decontaminate 833.33 L of acetaminophen-loaded water. Hence cost-performance ratio can be calculated using Eq. (6).

$$\text{Cost performance ratio} = \frac{C_{TZB}}{V} \quad (6)$$

The cost of fabricating the nanocomposite, including the amount of treated wastewater and the operational cost, is C_{TZB} ($170) and V (833.33 L), respectively. The cost-performance ratio is estimated at $0.204 L^{-1}. According to this finding, TZB may be employed as a productive and affordable adsorbent for the removal of acetaminophen from industrial wastewater.

4 Conclusions

This work uses TZB and TBC to investigate the sorption behaviour of acetaminophen from simulated wastewater under specific environmental conditions. When compared to TBC, the results indicated that TZB had a greater adsorption capability (q_e) for the adsorption operations. Because TiO_2/ZnO NPs enhanced the sorption of acetaminophen onto TZB's active sites, TZB's higher capacity was ascribed to their inclusion. Adsorption of acetaminophen was examined at pH 7, and for TBC and TZB, equilibrium was reached in 100 min, respectively. The adsorption kinetics for the uptake of acetaminophen onto TBC and TZB were best described by the pseudo-second-order model. The removal of acetaminophen was primarily brought about by π-electron-containing adsorbents and strong hydrophobic interactions. The Freundlich model provided a better description of the equilibrium data for the uptake of acetaminophen onto TBC and TZB. For the elimination of acetaminophen from an aqueous solution, an endothermic nature of adsorption was achieved, and all adsorption processes were feasible and spontaneous. TZB and TBC showed an endothermic nature in their elimination of acetaminophen. Entropy drives the sorption process. Good removal efficiencies were obtained by regeneration of acetaminophen-loaded adsorbents, suggesting that the adsorbents may be used again for related procedures. Since the adsorbents employed in this study were successful in removing acetaminophen, more research should be done to see how well they work for treating wastewater.

Acknowledgements The authors are grateful to VAAL University of Technology for support.

Author contribution James Amaku conceptualized the research, conducted laboratory experiments, analyzed the obtained data, and wrote the manuscript. Fanyana Mtunzi and Jesse Greener supervised, read, and edited the manuscript.

Funding Open access funding provided by Vaal University of Technology. This work has received support from the South African National Research Foundation (NRF, grant numbers PSTD23040188896).

Data availability Not applicable.

Declarations

Ethical approval Not applicable.

Consent to participate Not applicable.

Consent for publication All authors have studied the manuscript thoroughly and consented to the publication.

Competing interests The authors declare no competing interests.

References

1. Samal K, Mahapatra S, Ali MH (2022) Pharmaceutical wastewater as emerging contaminants (EC): treatment technologies, impact on environment and human health. Energy Nexus 6:100076
2. Khan S et al (2022) Emerging contaminants of high concern for the environment: current trends and future research. Environ Res 207:112609
3. Montaseri H, Forbes PB (2018) Analytical techniques for the determination of acetaminophen: a review. TrAC Trends Anal Chem 108:122–134

4. Lee W et al (2020) Removal of pharmaceutical contaminants from aqueous medium: a state-of-the-art review based on paracetamol. Arab J Sci Eng 45:7109–7135
5. Tatarchuk T, Soltys L, Macyk W (2023) Magnetic adsorbents for removal of pharmaceuticals: a review of adsorption properties. J Mol Liq 384:122174
6. Nibamureke UMC, Barnhoorn IEJ (2025) Screening of pharmaceuticals in surface waters from Vhembe District, Limpopo Province, South Africa. Water 17(3):379
7. Aljeboree AM, Alshirifi AN (2018) Adsorption of pharmaceuticals as emerging contaminants from aqueous solutions on to friendly surfaces such as activated carbon: a review. J Pharm Sci Res 10(9):2252–2257
8. Carvalho AP, Mestre AS, Haro M, Ania CO (2012) Advanced methods for the removal of acetaminophen from water. Acetaminophen: properties, clinical uses and adverse effects: Nova Science Publishers, pp 57–105
9. Matějová L et al (2022) Adsorption of the most common non-steroidal analgesics from aquatic environment on agricultural wastes-based activated carbons; experimental adsorption study supported by molecular modeling. Appl Surf Sci 605:154607
10. Rahman N et al (2021) Synthesis of 2-mercaptopropionic acid/hydrous zirconium oxide composite and its application for removal of Pb (II) from water samples: central composite design for optimization. Journal of King Saud University-Science 33(2):101280
11. Nasir M et al (2025) Statistical physics and fractal like kinetic modelling for adsorption of acetaminophen on MgO/aminated β-cyclodextrin: variables optimization using box-behnken design. J Ind Eng Chem. https://doi.org/10.1016/j.jiec.2025.01.030
12. Rahman N, Raheem A (2022) Fabrication of graphene oxide/inulin impregnated with ZnO nanoparticles for efficient removal of enrofloxacin from water: taguchi-optimized experimental analysis. J Environ Manage 318:115525
13. Rahman N, Varshney P (2021) Effective removal of doxycycline from aqueous solution using CuO nanoparticles decorated poly (2-acrylamido-2-methyl-1-propanesulfonic acid)/chitosan. Environ Sci Pollut Res Int 28(32):43599–43617
14. Quesada HB et al (2019) Acetaminophen adsorption using a low-cost adsorbent prepared from modified residues of *Moringa oleifera* Lam. seed husks. J Chem Technol Biotechnol 94(10):3147–3157
15. Moussavi G, Hossaini Z, Pourakbar M (2016) High-rate adsorption of acetaminophen from the contaminated water onto double-oxidized graphene oxide. Chem Eng J 287:665–673
16. Natarajan R et al (2021) Performance study on adsorptive removal of acetaminophen from wastewater using silica microspheres: kinetic and isotherm studies. Chemosphere 272:129896
17. Mashayekh-Salehi A, Moussavi G (2016) Removal of acetaminophen from the contaminated water using adsorption onto carbon activated with NH4Cl. Desalin Water Treat 57(27):12861–12873
18. Daikh S et al (2022) Equilibrium, kinetic and thermodynamic studies for evaluation of adsorption capacity of a new capacity hybrid adsorbent based on polyaniline and chitosan for acetaminophen. Chem Phys Lett 798:139565
19. Galhetas M et al (2014) Chars from gasification of coal and pine activated with K2CO3: acetaminophen and caffeine adsorption from aqueous solutions. J Colloid Interface Sci 433:94–103
20. Yanyan L et al (2018) Enhanced removal of acetaminophen from synthetic wastewater using multi-walled carbon nanotubes (MWCNTs) chemically modified with NaOH, HNO3/H2SO4, ozone, and/or chitosan. J Mol Liq 251:369–377
21. Alrefaee SH et al (2024) Removal of acetaminophen from wastewater using a novel bimetallic La/Th metal-organic framework: kinetics, thermodynamics, isotherms, and optimization through Box-Behnken design. Process Saf Environ Prot. https://doi.org/10.1016/j.psep.2024.06.046
22. Moacă E-A et al (2019) Fe3O4@ C matrix with tailorable adsorption capacities for paracetamol and acetylsalicylic acid: synthesis, characterization, and kinetic modeling. Molecules 24(9):1727
23. Geczo A et al (2021) Mechanistic insights into acetaminophen removal on cashew nut shell biomass-derived activated carbons. Environ Sci Pollut Res Int 28:58969–58982
24. Zyoud AH et al (2020) Removal of acetaminophen from water by simulated solar light photodegradation with ZnO and TiO2 nanoparticles: catalytic efficiency assessment for future prospects. J Environ Chem Eng 8(4):104038
25. Rajamehala M et al (2022) Synthesis of metal-based functional nanocomposite material and its application for the elimination of paracetamol from synthetic wastewater. Chemosphere 308:136530
26. Hasan M et al (2021) Biodegradation of salicylic acid, acetaminophen and ibuprofen by bacteria collected from a full-scale drinking water biofilter. J Environ Manage 295:113071
27. Draman SFS, Batra'azman IA, Mohd N (2015) Removal of paracetamol from aqueous solution by dried cellulose and activated carbon. ARPN J Eng Appl Sci 10:9544–9548
28. Patel M et al (2021) Ciprofloxacin and acetaminophen sorption onto banana peel biochars: environmental and process parameter influences. Environ Res 201:111218
29. Weber K, Quicker P (2018) Properties of biochar. Fuel 217:240–261
30. Wang J, Wang S (2019) Preparation, modification and environmental application of biochar: a review. J Clean Prod 227:1002–1022
31. Siddiqi KS et al (2018) Properties of zinc oxide nanoparticles and their activity against microbes. Nanoscale Res Lett 13:1–13
32. Adeniyi AG et al (2024) Leaf-based biochar: a review of thermochemical conversion techniques and properties. J Anal Appl Pyrolysis. https://doi.org/10.1016/j.jaap.2024.106352
33. Zhao B et al (2018) Effect of pyrolysis temperature, heating rate, and residence time on rapeseed stem derived biochar. J Clean Prod 174:977–987
34. Ortiz LR et al (2020) Influence of pyrolysis temperature and bio-waste composition on biochar characteristics. Renew Energy 155:837–847
35. Zhou J et al (2019) Bone-derived biochar and magnetic biochar for effective removal of fluoride in groundwater: effects of synthesis method and coexisting chromium. Water Environ Res 91(7):588–597
36. Jayawardhana Y et al (2019) Municipal solid waste-derived biochar for the removal of benzene from landfill leachate. Environ Geochem Health 41:1739–1753
37. Islam F et al (2022) Exploring the journey of zinc oxide nanoparticles (ZnO-NPs) toward biomedical applications. Materials 15(6):2160
38. Parihar V, Raja M, Paulose R (2018) A brief review of structural, electrical and electrochemical properties of zinc oxide nanoparticles. Rev Adv Mater Sci 53(2):119–130
39. Mondal NK, Basu S (2019) Capacityity of waste human hair towards removal of chromium (VI) from solution: kinetic and equilibrium studies. Appl Water Sci 9(3):49
40. Aksu Z, Karabayır G (2008) Comparison of biosorption properties of different kinds of fungi for the removal of Gryfalan Black RL metal-complex dye. Bioresour Technol 99(16):7730–7741
41. Sevim AM et al (2011) An investigation of the kinetics and thermodynamics of the adsorption of a cationic cobalt porphyrazine onto sepiolite. Dyes Pigments 88(1):25–38
42. Ofomaja A, Naidoo E, Modise S (2009) Removal of copper (II) from aqueous solution by pine and base modified pine cone powder as biosorbent. J Hazard Mater 168(2):909–917

43. Omorogie MO et al (2016) Clean technology approach for the competitive binding of toxic metal ions onto MnO2 nano-bioextractant. Clean Technol Environ Policy 18(1):171–184
44. Langmuir I (1918) The adsorption of gases on plane surface of glass, mica and platinum. J Am Chem Soc 40(9):1361–1403
45. Freundlich H (1906) Over the adsorption in solution. J Phys Chem 57(385):e470
46. Begum I et al (2022) A combinatorial approach towards antibacterial and antioxidant activity using tartaric acid capped silver nanoparticles. Processes 10(4):716
47. R Core Team (2016) R: A language and environment for statistical computing. R Foundation for Statistical Computing, Vienna. http://www.R-project.org/
48. Chia CH et al (2012) Imaging of mineral-enriched biochar by FTIR, Raman and SEM–EDX. Vib Spectrosc 62:248–257
49. Gonçalves NP et al (2022) Biochar waste-based ZnO materials as highly efficient photocatalysts for water treatment. J Environ Chem Eng 10(2):107256
50. Bhuyan MM et al (2018) Pectin-[(3-acrylamidopropyl) trimethylammonium chloride-co-acrylic acid] hydrogel prepared by gamma radiation and selectively silver (Ag) metal adsorption. J Appl Polym Sci 135(8):45906
51. Raheem A, Rahman N, Khan S (2024) Monolayer adsorption of ciprofloxacin on magnetic inulin/Mg–Zn–Al layered double hydroxide: advanced interpretation of the adsorption process. Langmuir 40(25):12939–12953
52. Nguyen DT et al (2020) Adsorption process and mechanism of acetaminophen onto commercial activated carbon. J Environ Chem Eng 8(6):104408
53. Rahman N, Ahmad I (2023) Insights into the statistical physics modeling and fractal like kinetic approach for the adsorption of As (III) on coordination polymer gel based on zirconium (IV) and 2-thiobarbituric acid. J Hazard Mater 457:131783
54. Saied ME et al (2024) Efficient adsorption of acetaminophen from the aqueous phase using low-cost and renewable adsorbent derived from orange peels. Biomass Convers Biorefin 14(2):2155–2172
55. Natarajan R, Kumar MA, Vaidyanathan VK (2022) Synthesis and characterization of rhamnolipid based chitosan magnetic nanosorbents for the removal of acetaminophen from aqueous solution. Chemosphere 288:132532
56. Nche N-AG et al (2017) Removal of paracetamol from aqueous solution by adsorption onto activated carbon prepared from rice husk. J Chem Pharm Res 9(3):56–68
57. Rahman N, Nasir M (2020) Effective removal of acetaminophen from aqueous solution using Ca (II)-doped chitosan/β-cyclodextrin composite. J Mol Liq 301:112454
58. Rahman N, Haseen U (2014) Equilibrium modeling, kinetic, and thermodynamic studies on adsorption of Pb (II) by a hybrid inorganic–organic material: polyacrylamide zirconium (IV) iodate. Ind Eng Chem Res 53(19):8198–8207
59. Doke KM, Khan EM (2013) Adsorption thermodynamics to clean up wastewater; critical review. Reviews in Environmental Science and Bio/Technology 12(1):25–44
60. Milonjić SK (2007) A consideration of the correct calculation of thermodynamic parameters of adsorption. J Serb Chem Soc 72(12):1363–1367
61. Nimse SB, Pal D (2015) Free radicals, natural antioxidants, and their reaction mechanisms. RSC Adv 5(35):27986–28006
62. Kehrer JP, Klotz L-O (2015) Free radicals and related reactive species as mediators of tissue injury and disease: implications for health. Crit Rev Toxicol 45(9):765–798
63. Azmi SNH et al (2021) Optimization for synthesis of silver nanoparticles through response surface methodology using leaf extract of *Boswellia sacra* and its application in antimicrobial activity. Environ Monit Assess 193(8):497
64. Balakrishnan A, Chinthala M (2024) Development of antibacterial biochar nanocomposite and its application in wastewater treatment. In: Biochar amendments for environmental remediation. CRC Press, pp 191–200. https://doi.org/10.1201/9781003344803-20
65. Leichtweis J et al (2023) Use of a new ZnFe2O4/biochar composite for degradation and ecotoxicity assessment of effluent containing methylene blue dye. J Photochem Photobiol A Chem 440:114676